An Assistive Strategy for Compliantly Actuated Exoskeletons using Non-Linear Model Predictive Control Method

S. M. Tahamipour-Z
Electrical Engineering Department,
Ferdowsi University of Mashhad
Mashhad, Iran.
Email: Tahamipourzarandi@mail.um.ac.ir

S. K. Hosseini Sani*
Electrical Engineering Department,
Ferdowsi University of Mashhad
Mashhad, Iran.
Email: k.hosseini@um.ac.ir

A. Akbarzadeh
Center of Excellence on Soft Computing and Intelligent Information Processing,
Mechanical Engineering Department,
Ferdowsi University of Mashhad,
Mashhad, Iran.
Email: Ali_Akbarzadeh@um.ac.ir

I. Kardan
Center of Excellence on Soft Computing and Intelligent Information Processing,
Mechanical Engineering Department,
Ferdowsi University of Mashhad
Mashhad, Iran
Email: Iman.Kardan@stu.um.ac.ir

***Abstract*— Assistive exoskeletons are a category of exoskeleton robots designed to provide extra powers and energies for elderlies or healthy subjects. The control algorithms of these robots, termed as assistive strategies, should control the robot in way that a portion of the user's required torques is provided by the robot actuators. This paper uses non-linear model predictive control (NMPC) method to propose a new assistive strategy for compliantly actuated exoskeletons. The user's required torques are estimated by using an identified model of the human-exoskeleton system. The NMPC method is then used to control the series elastic actuators of the robot to provide a user-selected portion of the estimated torques. The successful performance of the proposed assistive strategy is verified through multiple simulations. The force tracking performance of the NMPC method is also compared with a PID controller. The results clearly show the outperformance of the NMPC method in providing lower tracking errors and less control efforts.**

Keywords—Assistive control; Non-linear model predictive control; Series elastic actuators;

I. INTRODUCTION

Exoskeleton robots are increasingly used in different areas of the human life for easing the daily tasks of the users or providing them with some extra functionalities. According to [1], these robots are generally designed for one of the three main purposes of increasing the load carrying capabilities of the users [2], regenerating the lost mobilities for paralyzed patients [3] or providing extra powers and energies for elderlies or healthy subjects[4, 5]. The exoskeleton robots designed for the latter purpose are termed as assistive exoskeletons and their control algorithms are correspondingly termed as assistive strategies. An assistive strategy should control the robot to provide a portion of the required power for different motions of the user.

Various assistive strategies are proposed by the researchers [6-9]. However, most of the available strategies do not consider the saturation of the actuators as well as the possible disturbances which may act on the system. The exoskeleton robots are in contact with the human bodies and arbitrary motions of the users may act as some disturbances on the system. Therefore, an effective assistive strategy should be able to effectively reject the possible disturbances and should consider the saturation limits of the actuators. Some available assistive strategies such as the generalized assistive control framework by Oh et al. [10] and non-linear disturbance observer based control by Li et al. [11] consider the external disturbances but do not account for the saturation issue of the actuators.

Model predictive control (MPC) is a powerful control method which can readily account for the possible disturbances acting on the system and the saturation issue of the actuators. A model predictive controller predicts the future outputs of the system using a combination of measured states and applied control inputs. Considering the predicted outputs and their deviation from the desired values, the control inputs are then regulated to decrease the future errors. Following the three decades of development [12], the MPC method is currently found an increasing attention by the researchers and is largely applied to different dynamic systems [13-17]. The MPC method is also used for tracking control of the non-assistive upper limb [18] and lower limb [19] exoskeletons.

In this paper, a non-linear MPC (NMPC) method is used to develop an assistive strategy for a lower limb exoskeleton powered by series elastic actuators (SEA). The proposed strategy accounts for the measurable and un-measurable disturbances on the system and considers the limits on the control inputs to prevent the saturation of the actuators. To the best of the authors' knowledge, the NMPC method is not previously used in the available assistive strategies. The performance of the proposed assistive strategy is simulated for FUM-Physio robot built in robotics laboratory of the Ferdowsi

978-1-5386-4916-9/18/$31.00

University of Mashhad. A custom made series elastic actuator, called FUM-LSEA, is attached to the robot as a source of supplementary forces.

The rest of the paper is organized as follows; General outlines of the proposed assistive strategy is described in Section II. The SEA powered FUM-Physio robot is introduced in Section III and its dynamic model is derived. Section IV described the structure of the NMPC controller. The proposed assistive strategy is applied to the SEA powered FUM-Physio robot in Section V. Finally, Section VI concludes the paper.

II. PROPOSED ASSISTIVE STRATEGY

An assistive strategy should provide a portion of the torques required by the user joints in performing different tasks. Therefore, the required torque should be somehow estimated. Considering a rigid coupling between human and exoskeleton, the dynamic model of the so-called human-exoskeleton system, can be obtained as [20],

$$\mathbf{M}(\boldsymbol{\varphi})\ddot{\boldsymbol{\varphi}} + \mathbf{C}(\boldsymbol{\varphi}, \dot{\boldsymbol{\varphi}})\dot{\boldsymbol{\varphi}} + \mathbf{G}(\boldsymbol{\varphi}) = \boldsymbol{\tau}_h + \boldsymbol{\tau}_e \tag{1}$$

in which, $\boldsymbol{\varphi} \in \mathbf{R^n}$ is the vector of the generalized coordinates of the system, $\mathbf{M}(\boldsymbol{\varphi}) \in \mathbf{R^{n\times n}}$ is the mass matrix of the overall system, $\mathbf{C}(\boldsymbol{\varphi}, \dot{\boldsymbol{\varphi}})\dot{\boldsymbol{\varphi}} \in \mathbf{R^n}$ is the vector of the damping, centrifugal and Coriolis forces, $\mathbf{G}(\boldsymbol{\varphi}) \in \mathbf{R^n}$ is the vector of gravitational forces and $\boldsymbol{\tau}_h \in \mathbf{R^n}$ and $\boldsymbol{\tau}_e \in \mathbf{R^n}$ are the vectors of the torques applied by the user's joints and the actuators of the exoskeleton, respectively. The actuators should provide a portion of the torques required for the motions of the human-exoskeleton system. Therefore, the reference torque of the actuators can be written as,

$$\boldsymbol{\tau}_{er} = \alpha\left(\widehat{\mathbf{M}}(\boldsymbol{\varphi})\ddot{\boldsymbol{\varphi}} + \widehat{\mathbf{C}}(\boldsymbol{\varphi}, \dot{\boldsymbol{\varphi}})\dot{\boldsymbol{\varphi}} + \widehat{\mathbf{G}}(\boldsymbol{\varphi})\right) \tag{2}$$

where, $\widehat{\mathbf{M}}(\boldsymbol{\varphi})$, $\widehat{\mathbf{C}}(\boldsymbol{\varphi}, \dot{\boldsymbol{\varphi}})$ and $\widehat{\mathbf{G}}(\boldsymbol{\varphi})$ are the estimated dynamic matrices of the human-exoskeleton system and $\alpha \in [0,1]$ is the assistance coefficient. This constant determines the portion of the torques to be provided by the actuators.

Assuming an ideal torque controller, the actuator torques will instantly reach to their reference values. In other words, $\boldsymbol{\tau}_{\mathrm{e}} = \boldsymbol{\tau}_{\mathrm{er}}$. Substituting Eq.(2) in Eq.(1) the required human torques for the assisted motions can be calculated as,

$$\boldsymbol{\tau}_h = \left(\mathbf{M}(\boldsymbol{\varphi}) - \alpha\widehat{\mathbf{M}}(\boldsymbol{\varphi})\right)\ddot{\boldsymbol{\varphi}} + \left(\mathbf{C}(\boldsymbol{\varphi}, \dot{\boldsymbol{\varphi}}) - \alpha\widehat{\mathbf{C}}(\boldsymbol{\varphi}, \dot{\boldsymbol{\varphi}})\right)\dot{\boldsymbol{\varphi}} + \left(\mathbf{G}(\boldsymbol{\varphi}) - \alpha\widehat{\mathbf{G}}(\boldsymbol{\varphi})\right) \tag{3}$$

Eq.(3) clearly indicates that a better estimation of the dynamic matrices leads to a more accurate estimation of the assistive torques and a more effective assistance. Assuming a perfect estimation, the required human torques for the assisted motions simplify to,

$$\boldsymbol{\tau}_h = (1-\alpha)\big(\mathbf{M}(\boldsymbol{\varphi})\ddot{\boldsymbol{\varphi}} + \mathbf{C}(\boldsymbol{\varphi}, \dot{\boldsymbol{\varphi}})\dot{\boldsymbol{\varphi}} + \mathbf{G}(\boldsymbol{\varphi})\big) \tag{4}$$

Hence, in an ideal condition, by changing the value of the assistance coefficient from 0 to 1, the delivered assistance can be regulated between 0% and 100%.

Fig.(1) depicts a general scheme of the proposed algorithm in which $\mathbf{F}^*(\boldsymbol{\varphi})$ is a vector function relating the output force/torque of the actuators to the assisting torques applied to the system. Clearly, for rotary actuators which are connected to the joints through gearboxes, $\mathbf{F}^*$ is simply the vector of the gearboxes' ratios. However, in general, $\mathbf{F}^*$ is a function of the joint angles and depends on how the actuators are placed on the system. In the next section, $\mathbf{F}^*(\boldsymbol{\varphi})$ will be derived for the SEA powered FUM-Physio robot.

Output force of a series elastic actuator is a function of the spring deflection which is governed by both of the motor rotations and system motions. Therefore, considering the series elastic actuators as separate plants, the motion of the human-exoskeleton system will act as external disturbances to the SEA plants. This fact is also indicated in Fig.(1).

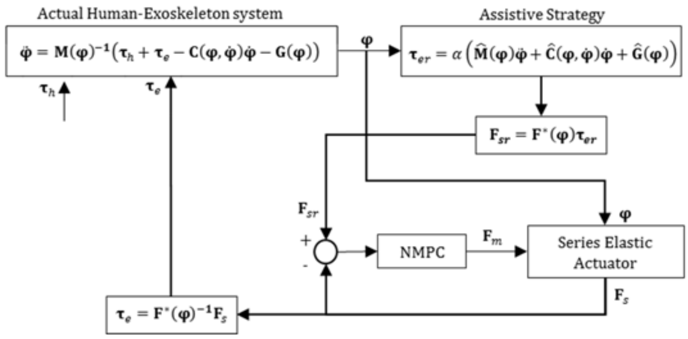

Fig. 1. Block diagram of the proposed assitive strategy.

Performing a good identification of the system, the dynamic matrices can be estimated by an acceptable error. Therefore, successful performance of the proposed strategy mostly depends on the quality of the torque controllers of the actuators. The exoskeleton robot is attached to the user's body. Consequently, arbitrary motions of the user act as external disturbances on the output torques of the actuators.

Regarding the nonlinearities in the system equations and the presence of the powerful disturbances, the nonlinear model predictive control method (NMPC) is used in this paper for regulating the actuators' torques. This method is well established for nonlinear and multi-DOF systems, readily accounts for the measurable and non-measurable disturbances on the system and takes care of the saturation of the actuators. Details of the NMPC controller are given in the Section IV.

III. FUM-PHYSIO ROBOBT

Fig.(2) shows FUM-Physio robot built in robotics laboratory of the Ferdowsi University of Mashhad. The main application of this robot is for automated knee rehabilitation. However, as shown in Fig.(2), FUM-Physio robot is designed in a way that a custom made series elastic actuator, FUM-LSEA, can be easily attached to the robot as a supplementary torque source. Therefore. FUM-Physio robot actuated by FUM-LSEA actuator can be considered as a single joint SEA powered exoskeleton. The arm of the robot represents a combination of the exoskeleton link and the user's leg while the servo motor of the robot represents the knee joint of the user. The torque required for following a given trajectory, τ_h, is provided by the servo motor of FUM-Physio. These assumptions are true as long as a rigid coupling is established between human limbs and exoskeleton links.

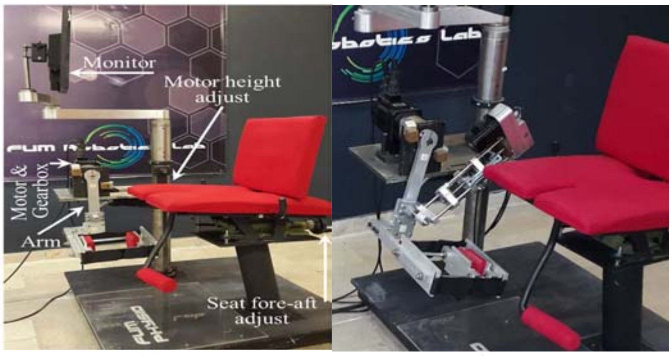

(a) (b)

Fig. 2. FUM-Physio robot; (a): FUM-Physio without SEA actuator, (b): FUM-Physio with FUM-LSEA as the suplementry force source [6].

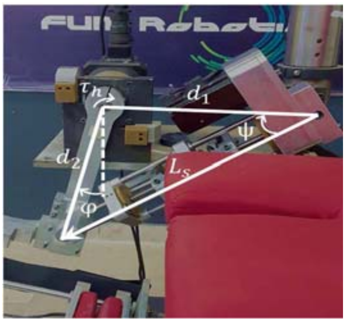

Fig. 3. Kinematic parameters of FUM-Physio robot actuated by FUM-LSEA.

Considering Fig.(3), the dynamic model of the system can be easily derived as,

$$\tau_h + \tau_e = I_p\ddot{\varphi} + B_p\dot{\varphi} + m_p g L_{gp}\sin(\varphi) \tag{5}$$

where, I_p is the rotary inertia of the arm, B_p is the damping coefficient of the robot joint, m_p is the mass of the arm and L_{gp} is the distance from center of gravity of the arm to the robot joint. According to Fig.(3), the output force of FUM-LSEA, F_s, applies an assistive torque to the arm as,

$$\tau_e = \mathrm{F}_s d_2\cos(\varphi)\cos(\psi) \tag{6}$$

in which,

$$\cos(\psi) = \frac{d_1^2 + L_S^2 - d_2^2}{2d_1 L_S} \tag{7}$$

L_s is

$$L_s = \sqrt{d_1^2 + d_2^2 - 2d_1 d_2\cos(\varphi)} \tag{8}$$

Using Eq.(6), $\mathrm{F}^*(\varphi)$ can be calculated as,

$$\mathrm{F}^*(\varphi) = \frac{1}{d_2\cos(\varphi)\cos(\psi)} \tag{9}$$

The output force of FUM-LSEA is function of the spring deflection and can be calculated as,

$$\mathrm{F_s} = K_s(y_m - \Delta L_s) + B_s(\dot{y}_m - \Delta\dot{L}_s) \tag{10}$$

where, K_s and B_s are the stiffness and damping of the spring used in the structure of FUM-LSEA and y_m is the linear displacement of the servo motor of the actuator. ΔL_s is the change in the length of FUM-LSEA calculated as,

$$\Delta L_s = L_s - \sqrt{d_1^2 + d_2^2} \tag{11}$$

The servo motor of the actuator should rotate the ball-screw, move the ball-screw nut, overcome the friction forces and deflect the spring. Therefore, the linear force of the servo motor of the actuator (linear equivalent of its torque) can be calculated as,

$$\mathrm{F_m} = M_m\ddot{y}_m + B_m\dot{y}_m + F_{cm}\mathrm{sign}(\dot{y}_m) + \mathrm{F}_s \tag{12}$$

in which, M_m, B_m and F_{cm} are respectively the equivalent linear mass, viscous friction coefficient and dry friction coefficient of the actuator parts geared to the servo motor. Eq.(12) defines the dynamic equation of the elastic actuator plant. F_m is the control input to the system and F_s is the system output which should be controlled to follow the desired value of,

$$\mathrm{F}_{sr} = \frac{\alpha}{d_2\cos(\varphi)\cos(\psi)}\left(I_p\ddot{\varphi} + B_p\dot{\varphi} + m_p g L_{gp}\sin(\varphi)\right) \tag{13}$$

Assuming an ideal force controller, $\mathrm{F}_s = \mathrm{F}_{sr}$, and substituting Eq.(13) and Eq.(6) in Eq.(5), the required torque for moving the assisted system can be obtained as,

$$\tau_h = (1-\alpha)\left(I_p\ddot{\varphi} + B_p\dot{\varphi} + m_p g L_{gp}\sin(\varphi)\right) \tag{14}$$

In an ideal condition, by setting the assistance coefficient to $\alpha = 1$, all the required torques are provided by FUM-LSEA and the given trajectories are followed with no effort. However, due to imperfections in identified system parameters and the tracking errors of the force controller, this condition will not hold in practice.

Using Eq.(10), the output force of FUM-LSEA can be divided into two separate parts as,

$$\mathrm{F}_s = \mathrm{F}_{sn} + \mathrm{F}_{sd} \tag{15}$$

where,

$$\mathrm{F}_{sn} = K_s y_m + B_s\dot{y}_m \tag{16}$$

$$\mathrm{F}_{sd} = -K_s\Delta L_s - B_s\Delta\dot{L}_s \tag{17}$$

F_{sn} is a function of the motions of the actuator motor and F_{sd} is a function of the system motions. Therefore, F_{sn} can be considered as the nominal output of the system and F_{sd} acts as an additive output disturbance. The arm angle φ can be measured by using the encoder of the servo motor of FUM-Physio robot and ΔL_s can be calculated using Eq.(11). Hence, F_{sd} is a measurable additive output disturbance.

IV. Non-Linear Model Predictive Control

Model predictive control method is based on optimizing the control effort, to minimize the future errors between actual and desired system outputs. This method uses a prediction horizon, n_p, and a control horizon, n_u, to form a dynamic matrix, $\mathbf{G}$, and calculate the future outputs of the system [21, 22], $\hat{\mathbf{F}}_s = [\mathrm{F}_s(k), \mathrm{F}_s(k+1), \dots, \mathrm{F}_s(k+n_p)]^T$.

$$\mathbf{G} = \begin{bmatrix} g_1 & 0 & \dots & 0 \\ g_2 & g_1 & \dots & 0 \\ \vdots & \vdots & \ddots & \vdots \\ g_{n_p} & g_{n_p-1} & \cdots & g_{n_p-n_u} \end{bmatrix} \quad (18)$$

where, g_i are calculated from impulse responses of the system. If the system under control is a linear system, $\mathbf{G}$ will be a constant matrix. However, in the case of a non-linear system, this matrix will not be constant. In such case the dynamic matrix is denoted as $\mathbf{G}|_k$ at k^{th} sampling instant. At each step the changes in the control signal, $\Delta\mathrm{F}_m(k) = \mathrm{F}_m(k) - \mathrm{F}_m(k-1)$, is calculated by minimizing the objective function J defined as,

$$\mathrm{J} = \sum_{i=1}^{n_p} \delta_i [\hat{\mathrm{F}}_s(k+i|k) - \mathrm{F}_{sr}(k+i)]^2 + \sum_{i=1}^{n_u} \lambda_i [\Delta\mathrm{F}_m(k+i-1)]^2 \quad (19)$$

in which δ_i and λ_i are the weights of the i^{th} sample of the output signal and control signal, respectively. In order to account for the saturation issue of the servomotors, the objective function should be minimized subjected to the following constraint.

$$\mathrm{F}_{m\,min} \leq \mathrm{F}_m \leq \mathrm{F}_{m\,max} \quad (20)$$

Solving the constrained minimization problem, the future changes in the control signal are obtained as,

$$\mathbf{\Delta F}_m = \left(\mathbf{G}|_k{}^T \mathbf{G}|_k + \lambda \mathbf{I}\right)^{-1} \mathbf{G}|_k{}^T (\mathbf{F}_{sr} - \hat{\mathbf{F}}_s) \quad (21)$$

in which, the future outputs of the system are obtained as,

$$\hat{\mathbf{F}}_s = \mathbf{G}|_k \, \Delta \mathbf{F}_m + \mathbf{F} \quad (22)$$

where,

$$\mathbf{F} = \mathbf{Y}_u + \mathbf{D}|_k \, \Delta\mathbf{Y}_d \quad (23)$$

In Eq.(23), $\mathbf{Y}_u$ is the system response to the control signal $\mathrm{F}_m(k)$, $\mathbf{D}|_k$ is a dynamic matrix similar to $\mathbf{D}|_k$ whose elements are the system response to impulsive disturbance inputs.

V. Simulation

In this section, the performance of the proposed assistive strategy is evaluated through implementation on the SEA actuated FUM-Physio robot. The identified parameters of the system are given in Table I. As given in Table I, the saturation limit on the output force of the servo motor of FUM-LSEA is set to $-1500(\mathrm{N}) \leq \mathrm{F}_m \leq 1500(\mathrm{N})$.

The MPC parameters are optimized by running multiple simulations and minimizing the integrated squared error (ISE) as the cost function. The ISE is calculated as,

$$\mathrm{ISE} = \int_0^T e_{(t)}^2 \, dt = \int_0^T \left(\mathrm{F}_{sr}(t) - \mathrm{F}_s(t)\right)^2 dt \quad (24)$$

Optimized control parameters are also given in Table I. Note that the control and prediction horizons should be chosen normally to maintain a desirable speed for the system.

Two different harmonic trajectories are considered for the φ angle. The first trajectory, called Taj.I, is a biased sinusoidal motion with a frequency of $\omega = 1(rad/s)$. The second trajectory, called Traj.II, is a summation of four harmonic motions with different frequencies and phases. Mathematical definitions of these trajectories are given in Eq.(25) and Eq.(26) and depicted in Fig.(4).

TABLE I. Parameter values

System Parameters		NMPC		PID	
Parameter	*value*	*Parameter*	*value*	*Parameter*	*value*
$M_m\ (kg)$	1673.9	T_s (s)	0.001	P	800
$B_m(Ns/m)$	900	n_p	5	I	26
$B_s(Ns/m)$	2.56	n_u	3	D	20
$K_s(N/m)$	8600	λ_i	0.045		
$m_p g L_{gp}\ (Nm)$	12.61	δ_i	222.5		
$I_p(kgm^2)$	0.53				
$B_p(Nms/rad)$	3.31				
$d_1(m)$	0.29				
$d_2(m)$	0.23				

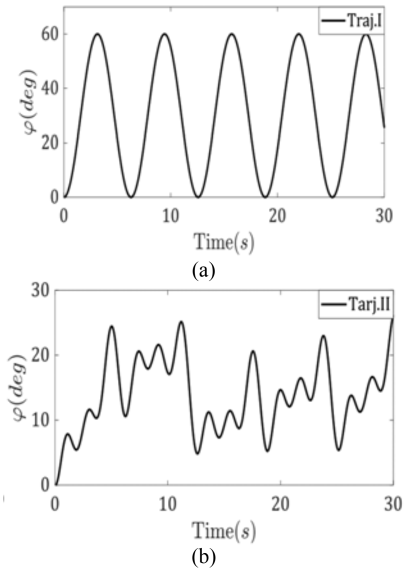

Fig. 4. Given trajectories for evaluation of the proposed assistance strategy; (a): Traj.I, (b): Traj.II.

$$\text{Traj.I:} \qquad \varphi = \pi/6\left(\sin\left(\mathrm{w}t + \frac{\pi}{2}\right) - 1\right) \quad (25)$$

$$\text{Traj.II: } \varphi = -3/50\left(\cos\left(\frac{3\pi}{20} + 3t\right) + \cos\left(\frac{\pi}{40} + \frac{t}{3}\right) + \sin\left(\frac{11\pi}{40} + 0.5t\right) + \sin\left(\frac{2\pi}{5} + 2t\right) + \sin\left(\frac{3\pi}{20} + t\right)\right) \quad (26)$$

Setting different values of $\alpha = 0.3$, $\alpha = 0.5$ and $\alpha = 0.65$ for the assistance coefficient, the required torques for the trajectories Traj.I and Traj.II are depicted in Fig.(5).

The torque trajectories in Fig.(5) clearly indicate the successful performance of the proposed assistive strategy in assisting the system and reducing the required torques. It is also evident that increasing the assistance coefficient, effectively reduces the required torques for a fixed trajectory.

Fig.(6) compares the force tracking performance of the NMPC force controller with a PID controller. The coefficients of the PID controller are also optimized by using the ISE cost function and running multiple simulations. Two harmonic trajectories are applied to the system and the reference force trajectories for the actuators are calculated form Eq.(13). The first applied trajectory is the previously defined Taj.I with $\omega = 1(rad/s\,)$. The second trajectory is also similar to Traj.I but with a higher frequency of $\omega = 3(rad/s)$, called Traj.III.

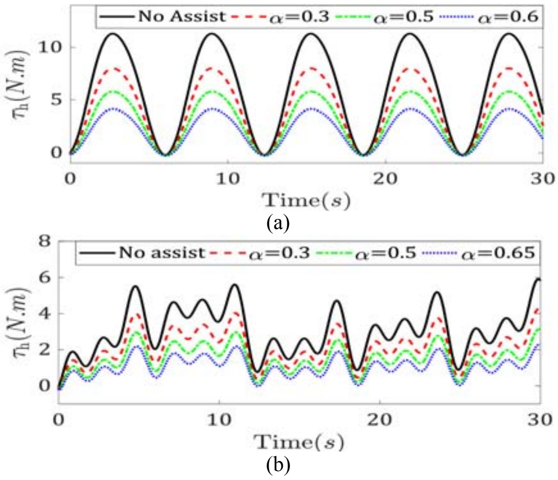

Fig. 5. Required user torques for different values of the assistance coefficient; (a): Traj.I, (b): Traj.II.

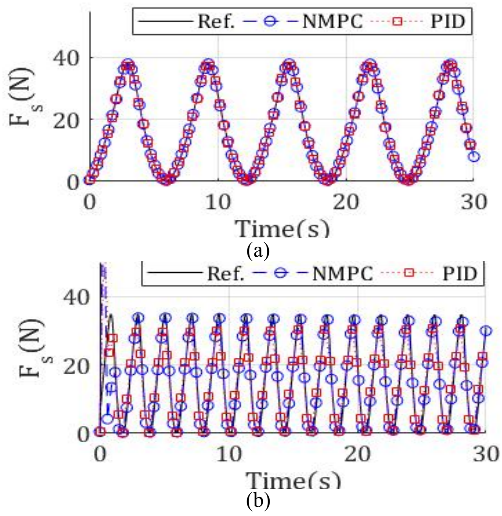

Fig. 6. (b) Force tracking performance of the NMPC method compared with PID controller; (a): Traj.I, (b): Traj.III.

Fig.(7) depicts the force tracking errors for the two trajectories. It is clear that although both of the controllers provide similar performances in the low frequency trajectory, the NMPC method provides visibly lower tracking errors for the trajectory with higher frequency.

Fig.(8) compares the control effort, F_m, of the NMPC method to that of the PID controller. It is clear that for both of the low and high frequency trajectories, the NMPC method requires less control effort. The outperformance of the NMPC method is better justified in the case of the high frequency trajectory. In this case, the PID controller completely saturates the servomotor of the FUM-LSEA.

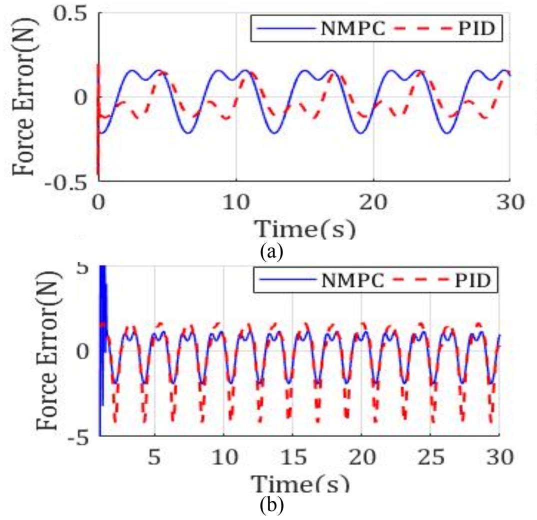

Fig. 7. Force tracking Error of the NMPC method compared with PID controller; (a): Traj.I, (b): Traj.III.

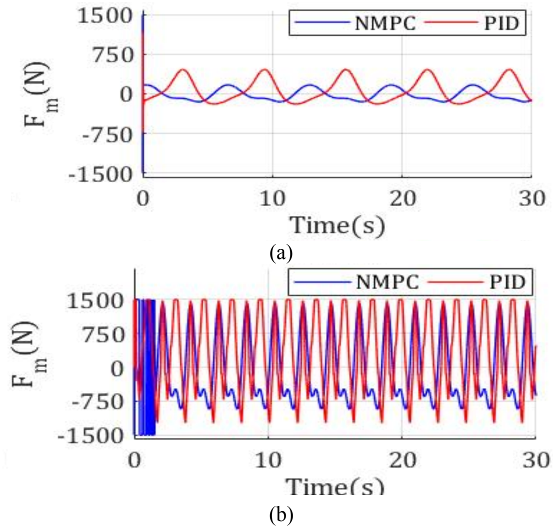

Fig. 8. Control effort of the NMPC method compared with PID controller; (a): Traj.I, (b): Traj.III.

The provided results clearly indicate that by using the NMPC method, the reference force trajectory is tracked with small errors while the external disturbances are successfully rejected and the servomotors of the actuators are effectively protected from being saturated.

VI. Conclusion

In this paper, an assistive control strategy is proposed for compliantly actuated exoskeletons. The proposed strategy controls the motors of the series elastic actuators to provide a user-selected portion of the required torques. Therefore, lower torques should be provided by the user's joints and different motions could be performed with less efforts from the user. NMPC method is used as the force controller to adjust the output force of the elastic actuators. This method readily considers the measurable and unmeasurable disturbances and accounts for the saturation issue of the actuator. The provided results clearly indicate the successful performance of the proposed assistive strategy in decreasing the required user's torques, hence assisting his/her motions. The force tracking performance of the NMPC method is also evaluated and compared to that of a PID controller. The results show that comparing to the PID controller, NMPC method provides lower tracking errors and requires less control efforts. The outperformance of the NMPC method is particularly more evident in high frequency motions where the NMPC method provides visibly lower tracking errors. Moreover, the PID controller may saturate the actuators in a high frequency motion while the NMPC method successfully prevents the actuators from being saturated.

REFERENCES

[1] T. Yan, M. Cempini, C. M. Oddo, and N. Vitiello, "Review of assistive strategies in powered lower-limb orthoses and exoskeletons," Robotics and Autonomous Systems, vol. 64, pp. 120-136, 2015.

[2] Z. Yang, W. Gu, J. Zhang, and L. Gui, "Force Control Theory and Method of Human Load Carrying Exoskeleton Suit," ed: Springer, 2017.

[3] K. H. Ha, S. A. Murray, and M. Goldfarb, "An approach for the cooperative control of FES with a powered exoskeleton during level walking for persons with paraplegia," IEEE Transactions on Neural Systems and Rehabilitation Engineering, vol. 24, no. 4, pp. 455-466, 2016.

[4] O. Jansen et al., "Hybrid assistive limb exoskeleton HAL® in the rehabilitation of chronic SCI: Proof of concept, the results of 21 patients," World neurosurgery, 2017.

[5] H. Kazerooni, R. Steger, and L. Huang, "Hybrid Control of the Berkeley Lower Extremity Exoskeleton (BLEEX)," Int. J. Rob. Res., vol. 25, no. 5-6, pp. 561-573, 2006.

[6] I. Kardan, I. Kardan, A. Akbarzadeh, and A. Akbarzadeh, "Output feedback assistive control of single-DOF SEA powered exoskeletons," Industrial Robot: An International Journal, vol. 44, no. 3, pp. 275-287, 2017.

[7] I. Kardan and A. Akbarzadeh, "Robust output feedback assistive control of a compliantly actuated knee exoskeleton," Robotics and Autonomous Systems, vol. 98, pp. 15-29, 2017.

[8] W. Huo, S. Mohammed, Y. Amirat, and K. Kong, "Active impedance control of a lower limb exoskeleton to assist sit-to-stand movement," in Robotics and Automation (ICRA), 2016 IEEE International Conference on, 2016, pp. 3530-3536: IEEE.

[9] S. Lee and Y. Sankai, "Power assist control for leg with hal-3 based on virtual torque and impedance adjustment," in Systems, Man and Cybernetics, 2002 IEEE International Conference on, 2002, vol. 4, p. 6 pp. vol. 4: IEEE.

[10] S. Oh, E. Baek, S.-k. Song, S. Mohammed, D. Jeon, and K. Kong, "A generalized control framework of assistive controllers and its application to lower limb exoskeletons," Robotics and Autonomous Systems, vol. 73, pp. 68-77, 2015.

[11] Z. Li, C.-Y. Su, L. Wang, Z. Chen, and T. Chai, "Nonlinear disturbance observer-based control design for a robotic exoskeleton incorporating fuzzy approximation," IEEE Transactions on Industrial Electronics, vol. 62, no. 9, pp. 5763-5775, 2015.

[12] J. H. Lee, "Model predictive control: Review of the three decades of development," International Journal of Control, Automation and Systems, journal article vol. 9, no. 3, p. 415, June 04 2011.

[13] V. R. Desaraju and N. Michael, "Leveraging experience for computationally efficient adaptive nonlinear model predictive control," in Robotics and Automation (ICRA), 2017 IEEE International Conference on, 2017, pp. 5314-5320: IEEE.

[14] R. González, M. Fiacchini, J. L. Guzmán, T. Álamo, and F. Rodríguez, "Robust tube-based predictive control for mobile robots in off-road conditions," Robotics and Autonomous Systems, vol. 59, no. 10, pp. 711-726, 2011/10/01/ 2011.

[15] A. Ferrara, G. P. Incremona, and L. Magni, "A robust MPC/ISM hierarchical multi-loop control scheme for robot manipulators," in Decision and Control (CDC), 2013 IEEE 52nd Annual Conference on, 2013, pp. 3560-3565: IEEE.

[16] D. Gu and H. Hu, "Neural predictive control for a car-like mobile robot," Robotics and Autonomous Systems, vol. 39, no. 2, pp. 73-86, 2002/05/31/ 2002.

[17] A. M. Jasour and M. Farrokhi, "Path tracking and obstacle avoidance for redundant robotic arms using fuzzy NMPC," in American Control Conference, 2009. ACC'09., 2009, pp. 1353-1358: IEEE.

[18] J. Hu, X. Xu, and K. Zhu, "Arm Exoskeleton Based on Model Predictive Control with Input/Output Feedback Linearization," Journal of Medical Imaging and Health Informatics, vol. 3, no. 3, pp. 432-439, 2013.

[19] C. A. Rodriguez, P. Ponce, and A. Molina, "ANFIS and MPC controllers for a reconfigurable lower limb exoskeleton," Soft Computing, vol. 21, no. 3, pp. 571-584, 2017.

[20] M. W. Spong, S. Hutchinson, and M. Vidyasagar, Robot modeling and control. Wiley New York, 2006.

[21] C. R. Cutler and B. L. Ramaker, "Dynamic matrix control?? a computer control algorithm," in Joint automatic control conference, 1980, no. 17, p. 72.

[22] P. Guzmicky and S. Kozak, "Dynamic matrix control of thermal-optical laboratory System," in CONTROLO’2012, 2012.